Physica Medica 66 (2019) 88–96

Contents lists available at ScienceDirect

Physica Medica

journal homepage: www.elsevier.com/locate/ejmp

Original paper

External photon radiation treatment for prostate cancer: Uncomplicated and cancer-free control probability assessment of 36 plans

B. Sánchez-Nieto[a,*], M. Romero-Expósito[b], J.A. Terrón[c], L. Irazola[d], M.T. García Hernández[e], J.C. Mateos[d,f], J. Roselló[e,g], D. Planes[e], M. Paiusco[h], F. Sánchez-Doblado[c,d]

[a] Instituto de Física, Pontificia Universidad Católica de Chile, Santiago, Chile
[b] Departament de Física, Universitat Autónoma de Barcelona, Bellaterra, Spain
[c] Hospital Universitario Virgen Macarena, Sevilla, Spain
[d] Departamento de Fisiología Médica y Biofísica, Universidad de Sevilla, Sevilla, Spain
[e] ERESA, Valencia, Spain
[f] Hospital Universitario Virgen del Rocío, Sevilla, Spain
[g] Departamento de Fisiología, Universidad de Valencia, Spain
[h] Veneto Institute of Oncology IOV – IRCCS, Padua, Italy

ARTICLE INFO

Keywords:
Prostate radiotherapy treatment
Radiobiological modelling
Second primary cancer risk
Radiotherapy plan optimisation
Tumour control probability
Normal tissue complication probability
Radiation protection of the patient

ABSTRACT

Purpose: To perform a systematic and thorough assessment, using the Uncomplicated and Cancer-Free Control Probability (UCFCP) function, of a broad range of photon prostate cancer RT treatments, on the same scenario (a unique pelvic CT set). UCFCP considers, together with the probabilities of local tumour control (TCP) and deterministic (late) sequelae (NTCP), the second primary cancer risk (SPCR) due to photon and neutron peripheral doses.

Methods and materials: Thirty-six radiotherapy plans were produced for the same CT. 6, 10, 15 and 18 MV 3DCRT, IMRT and VMAT (77.4 Gy in 43 fractions) and 6 and 10 MV SBRT (36.25 Gy in 5 fractions with flattened and FFF beams) for Elekta, Siemens and Varian Linacs plans were included. DVH and peripheral organ dosimetry were used to compute TCP, NTCP, and SPCR (the competition and LNT models) for further plan ranking.

Results: Biological models (and parameters) used predicted an outcome which is in agreement with epidemiological findings. SBRT plans showed the lowest SPCR and a below average $NTCP_{rectal}$. High energy plans did not rank worse than the low energy ones. Intensity modulated plans were ranked above the 3D conformal techniques.

Conclusions: According to UCFCP, the best plans were the10 MV SBRTs. SPCR rates were low and did not show a substantial impact on plan ranking. High energy intensity-modulated plans did not increase in excess the average of SPCR. Even more, they ranked among the best, provided that MU were efficiently managed.

1. Introduction

Based on data from Surveillance, Epidemiology, and End Results Program (SEER) 2012–2014 (https://seer.cancer.gov/statfacts/html/prost.html), approximately 11.6% of men in the US will be diagnosed with prostate cancer (PoCa) at some point during their lifetime, with 174.650 estimated new cases in 2019 (https://cancerstatisticscenter.cancer.org). The high prevalence of PoCa and the reduction in mortality after radiotherapy (RT) [1], make the radiation-induced second primary cancers, due to out-of-field photon and neutron doses, particularly relevant. The latter must be borne in mind when considering which patients to irradiate and which techniques to employ [2].

Photon radiation-based treatments which are available worldwide for PoCa are very versatile. Intensity-modulated RT (IMRT) techniques were implemented to improve the conformality of the dose distribution further, compared to three-dimensional conformal RT (3D-CRT) [3], and thereby facilitate dose escalation while keeping (or even decreasing) the toxicity of surrounding organs [4]. More recently, Stereotactic Body Radiotherapy (SBRT) has emerged as a procedure characterised by delivering large doses in a few fractions [5,6].

The quality of RT plans has been traditionally judged by physical quantities (i.e., dose and dose-volume parameters). However, those metrics should be replaced by biological indexes (e.g., Tumor Control Probability -TCP- and Normal Tissue Complication probability -NTCP-)

* Corresponding author at: Instituto de Física, Pontificia Universidad Católica de Chile, Avenida Vicuña Mackenna 4860, Macul, Santiago, Chile.
E-mail address: bsanchez@fis.puc.cl (B. Sánchez-Nieto).

https://doi.org/10.1016/j.ejmp.2019.09.076
Received 16 July 2019; Received in revised form 18 August 2019; Accepted 11 September 2019
Available online 29 September 2019
1120-1797/ © 2019 Associazione Italiana di Fisica Medica. Published by Elsevier Ltd. All rights reserved.

for the treatment process to more closely reflect the clinical goals of RT [7]. Along this line, the mentioned concern on second cancers, especially for the photon modern RT techniques (e.g., IMRT or Volumetric Modulated Arc Therapy – VMAT) [8–12] could be of particular importance among long-term cancer survivors such as PoCa patients. Thus, the quality of RT plans should be judged in terms of TCP as well as of the risk of normal-tissue toxicity, both stochastic and deterministic events. To confront this issue, a biological model to evaluate the success of the treatments (Uncomplicated and Cancer-Free Control Probability-UCFCP), taking into consideration the risk of deterministic (late) sequelae (NTCP) and second primary cancer risks (SPCR[1]), has been proposed [13].

In summary, there is a variety of PoCa irradiation techniques, but the impact on second primary cancers, which are an uncommon but a severe consequence of RT especially when treating younger patients, is uncertain [14]. And yet, probably due to the lack of adequate tools for a balanced analysis, the use of, for example, high energy photons is neglected beforehand. Therefore, this paper aimed to evaluate, in a systematic way and through UCFCP, the expected outcome associated with a pool of different available photon irradiation options. To make a fair comparison among techniques, they were applied to the same patient anatomy. In this way, this papers describes a methodology which could be followed for the choice of the best prostate plan, among the techniques (or energies) available in a specific clinic. To our knowledge, it is the first time that such a thorough analysis comprising not only TCP but possible toxicities associated with photon and neutron doses deposited outside the treatment volume has been performed.

2. Methods and materials

2.1. Radiotherapy plans

The CT set used in the study corresponds to the anonymised planning CT set of an RT patient. The patient signed an informed consent form on the potential use of the anonymised images for research purposes.

Thirty-six prostate RT plans (Table 1) were created on the same patient CT and organs contours set (avoiding inter-operator OAR contouring variability). The CT set (together with GTV, PTV, rectum and bladder contours) was sent to each of the seven participating RT centres who provided plans covering a broad spectrum of standard and hypofractionated (3D-CRT, forward IMRT, inverse IMRT, VMAT and SBRT) photon beam techniques for low (6MV) and high (10, 15 and 18MV) energy, flattened and unflattened (FFF) beams using the Elekta, Siemens, and Varian linacs. All SBRT plans were provided by the same centre and were designed using VMAT.

Participating centres provided their optimum plan according to their resources. GTV (gland without seminal vesicles) and PTV (except for SBRT) volumes were distributed to the participating centres together with the contoured nearby organs at risk (rectum, from rectosigmoid junction to anus, and bladder contoured as solid organs). Planners were asked to cover 95% of PTV with 95% of the phase I prescription dose (59.4 Gy in 1.8 Gy/fr) and to boost the GTV with 18 Gy in 1.8 Gy/fr (at least 95% of GTV covered with 95% boosting dose). SBRTs were aimed to cover the PTV (3 mm isotropic margins around GTV) with 95% of the prescription dose (36.25 Gy in 7.25 Gy/fr). Fig. 1 depicts all DVHs for PTV, rectum, and bladder. 1.8 Gy/fr plans met recommended constraints [15] for rectum (except VVM6 and S3D18 with V_{75} = 4% instead of 3%), and the QUANTEC recommended dose-volume limits for bladder [16]. All SBRTs fulfilled the same biologically corrected dose constraints (calculated with α/β = 3 Gy).

Table 1
Description of the 36 external photon beam radiation treatments.

Technique	Energy	Linac Manufacturer		
	(MV)	Elekta (E)	Siemens (S)	Varian (V)
3D-CRT (3D)	6	X	X	X
	10	X		
	15	X	X	X
	18	X	X	X
Forward IMRT (IM*f*)	6		X	X
	15		X	X
	18		X	
Inverse IMRT (IM*i*)	6	X	X	X
	10	X		
	15	X	X	X
	18	X	X	X
VMAT (VM)	6	X		X
	10	XX		
	15	X		X
	18	X		
SBRT (SB)	6			XX
	10			XX

In the first column, abbreviations used in the text/table and figures to identify each RT technique are indicated in brackets. *f* and *i* are for forward and inverse planning, respectively. Each linac manufacturer is identified by its first letter (E, S or V). XX means two plans available: single/double arcs for VMAT and FF/FFF for SBRT. Plans are named with the following code: the first letter indicates the linac, then the technique and finally the energy.

3. Biological indexes

The Uncomplicated and Cancer-Free Control Probability (UCFCP) model was proposed by Sánchez-Nieto et al. [13]. This function assumes a statistically uncorrelated dose response for tumour and normal tissues and when both are equally weighted (see discussion), it can be expressed as:

$$UCFCP = TCP \cdot \prod_{i=1}^{n} (1 - NTCP_i) \cdot (1 - SPCR) = TCP \cdot (1 - NTCP_{tot}) \cdot (1 - SPCR) \quad (1)$$

where $NTCP_i$ with $i = 1,\ldots n$ is the probability of late toxicity in an *i-th* nearby organ and the overall $NTCP_{tot}$ can be found from $1 - \prod_{i=1}^{n} (1 - NTCP_i)$ where there are as many products terms as there are normal tissues considered (rectum and bladder in the case of this exercise).

If now TCP and $NTCP_{tot}$ are gathered under the "classical" Uncomplicated tumour Control Probability (UCP) [17], UCFCP can be finally expressed as:

$$UCFCP = UCP \bullet (1 - SPCR) \quad (2)$$

Moreover, the Global Complication Probability (GCP) dose–response function, comprising both, the chance of suffering any normal tissue toxicity (i.e., $NTCP_{tot}$) and SPCR, can also be used to express the UCFCP as follows:

$$UCFCP = TCP \bullet (1 - SPCR - \mathrm{NTCPtot} - SPCR \bullet \mathrm{NTCPtot}) = TCP \cdot (1 - GCP) \quad (3)$$

For each of the 36 plans, UCFCP was computed using eq.1. TCP (Poisson model for GTV as in [18]) and NTCP (LKB model [19,20] for rectum and bladder) values were calculated with BIOPLAN [17] with parameters from [21,22] (Table 2). SPCR was calculated as the summation over risks values, given by the Life Attributable Risk (LAR), of the peripheral organs in BEIR VII PHASE 2 report [23] (lung, stomach, thyroid, red marrow[2], colon, bladder, liver, skin, rectum and the

[1] SPCR was named as SCP in [13]

[2] Active bone marrow is mainly distributed among the spine, pelvis and rib

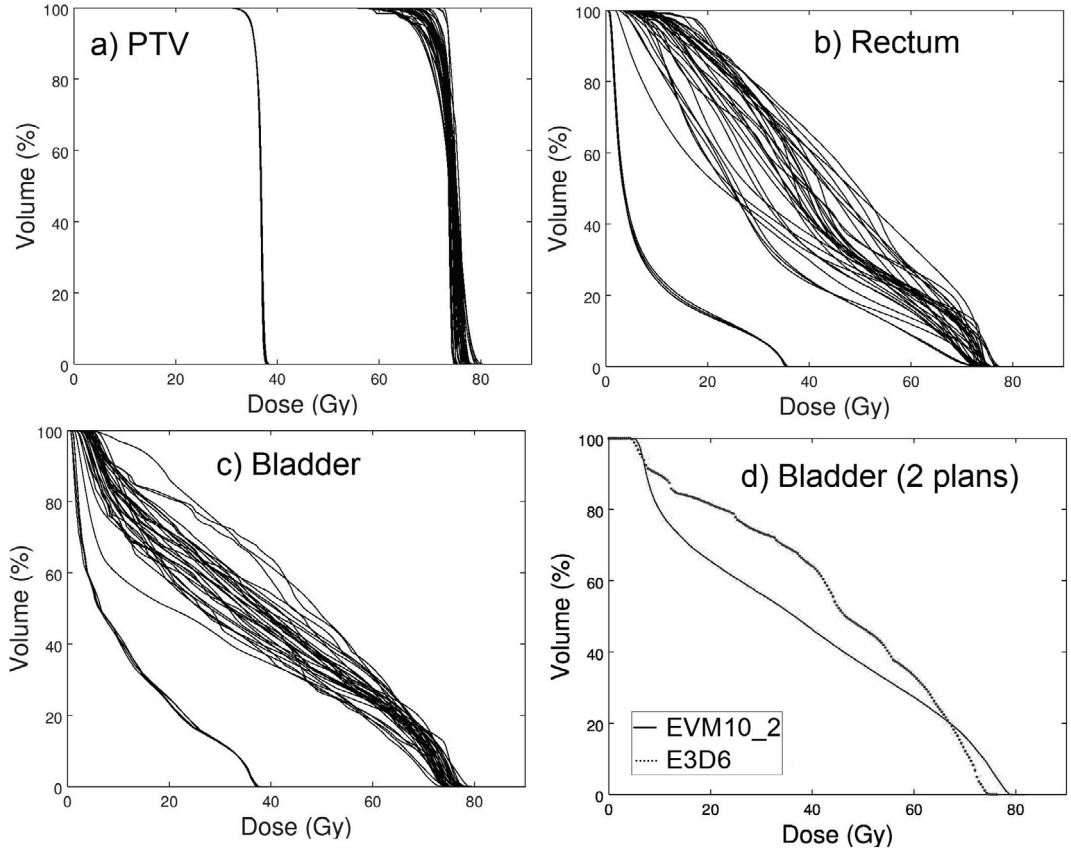

Fig. 1. PTV(a), rectum(b) and bladder(c) DVHs for all plans. SBRT margin reduction from GTV to PTV increases rectal and bladder sparing. Subfigure (d) depicts DVH plans with extreme $NTCP_{bladder}$ values (10.8% for EVM10_2 and 0% for E3D6) to illustrate the impact to bladder toxicity of volumes irradiated to high doses.

remainder).

The calculation of LAR requires prior knowledge of the dose to the out-of-field (i.e., peripheral) organs. Depending on the distance to the field edge, two regions were considered for which the peripheral photon dose information available was different and so the methodology to calculate LAR. Specifically, 50% and 5% isodoses were used to delimit the boundary for the medium- and low- dose regions [13].

For organs located within the medium-dose region (between the 50% and 5% isodoses), such as the rectum and a portion of the bladder, DVH information provided by the treatment planning systems (TPS) were transformed into Organ Equivalent Dose (OED) [24,25] through organ-specific dose–response mechanistic models as follows:

$$OED = \frac{1}{V_T}\sum_i V(D_i)\cdot RED(D_i) = \frac{1}{V_T}\sum_i V(D_i)\cdot\frac{e^{-\alpha'\cdot D_i}}{\alpha'\cdot R}\left(1-2R+R^2\cdot e^{\alpha'\cdot D_i}-(1-R)^2\bullet e^{-\frac{\alpha'\cdot R}{1-R}\cdot D_i}\right) \quad (4)$$

where $V(D_i)$ represents the DVH, V_T the total volume of the organ, and $RED(D_i)$ the dose-response relationship for radiation induced cancer of the organ [26]. Finally, R characterises the repopulation/repair-ability of the tissue between two dose fractions and α' is defined from the radiobiological parameters α and β as follows:

$$\alpha' = \alpha + \beta\frac{D}{D_T}d_T \quad (5)$$

Table 2
Parameters (with references) used for TCP, NTCP and SPCR calculations.

Dose-response model	Parameters	
$TCP_{Poisson}$	$\alpha = 0.29\,Gy^{-1}$ $\sigma_\alpha = 0.07\,Gy^{-1}$ $\alpha/\beta = 3\,Gy$ $\rho_c = 10^7 cells/cm^3$	
NTCP-LKB	Rectum bleeding or RTOG grade ≥ 2 (Michaslki *et al.*, 2010) TD50 = 76.9 Gy m = 0.13 n = 0.09 α/β = 3Gy[a] Rectum (Schneider et al., 2011)[b]	Bladder Grade ≥ 1 toxicity within 2 years (Cheung *et al.*, 2007) TD50 = 77.6 Gy m = 0.022 n = 0.00995 α/β = 3Gy[a] Bladder (Schneider *et al.*, 2011)
SPCR (mechanistic model for the medium-dose region)	$\alpha_{bladder} = 0.219\,Gy^{-1}$ α/β = 3 Gy R = 0.56 $\beta_{EAR\text{-}UK} = 0.73$ $\gamma_e = -0.056$ $\gamma_a = 6.9$	$\alpha_{rectum} = 0.033\,Gy^{-1}$ α/β = 3 Gy R = 0.06 $\beta_{EAR\text{-}UK} = 3.8$ $\gamma_e = -0.024$ $\gamma_a = 2.38$

TD50 whole organ dose for which NTCP is 50%.
m is a dimensionless parameter reflecting the heterogeneity of TD50 values.
n is the volume parameter.
α, β and α/β come from the LQ model.
R characterises the repopulation/repair-ability of the tissue between two dose fractions.

[a] For Linear-Quadratic -LQ- correction of doses (for the case of bladder equivalent dose in 1.8 Gy/# was only applied to hypofractionated DVD)

[b] See the separate erratum for rectal coefficients in https://tbiomed.biomedcentral.com/articles/10.1186/1742–4682-8–27/comments

(*footnote continued*)
cage. Average dose to these organs was consired as representative of dose to bone marrow.

Table 3
Biological indexes calculated for all the plans*. SPCR, GCP and UCFCP, which depend on the age at exposure, were calculated for 60 and 80 years, but plans are ranked according to the UCFCP value at 60 years. Three equally-sized groups were created, and, additionally, the number of MU of each plan was included. All values were rounded to one decimal, but the ranking in terms of UCFCP considered up to 2 decimals.

Plans		Biological Indexes (in %) independent on age at exposure				Biological Indexes (in %) dependent on age at exposure					
		MU				60 years			80 years		
			TCP	$NTCP_{rectum}$	$NTCP_{bladder}$	*UCP*	*SPCR*	*GCP*	*UCFCP*	*SPCR*	*GCP*	*UCFCP*
	VSB10	1890	98.0	0.8	0.9	96.3	1.1	2.8	95.3	0.24	1.9	96.1
	VSB10_fff	2341	97.8	0.8	0.8	96.2	1.1	2.7	95.2	0.92	2.5	95.4
	VSB6_fff	2730	97.8	0.7	1.2	96.0	1.1	2.9	94.9	0.41	2.3	95.6
	VIMf6	18,348	96.1	0.3	0.6	95.2	2.2	3.0	93.2	0.76	1.7	94.5
	VIMf15	14,233	96.4	0.3	0.8	95.3	2.4	3.5	93.1	0.9	2.0	94.5
I	*VIMi6*	33,422	96.0	0.8	0.2	95.0	2.1	3.1	93.0	0.82	1.8	94.3
	SIMf15	12,052	96.1	0.9	0.2	95.0	2.2	3.3	93.0	0.86	2.0	94.2
	E3D18	9805	96.2	1.4	0.0	94.9	2.1	3.5	92.8	0.83	2.2	94.1
	EIMi10	11,763	96.5	1.6	0.5	94.5	2.0	4.1	92.6	0.81	2.9	93.7
	E3D10	11,096	96.3	1.9	0.0	94.5	2.0	3.9	92.5	0.81	2.7	93.7
	SIMi15	15,265	95.8	0.8	0.5	94.6	2.2	3.4	92.5	0.87	2.2	93.7
	EVM18_1	9644	96.0	1.6	0.0	94.5	2.1	3.7	92.5	0.84	2.4	93.7
	VIMi15	15,365	95.9	0.9	0.2	94.8	2.5	3.6	92.5	0.93	2.0	94
	SIMi6	17,744	95.9	0.9	0.9	94.2	2.1	3.8	92.2	0.84	2.6	93.4
	SIMi18	22,270	95.6	1.4	0.0	94.3	2.2	3.6	92.2	0.91	2.3	93.4
	E3D15	10,337	95.8	1.9	0.0	94.0	2.1	3.9	92.0	0.83	2.7	93.2
	VSB6	2350	98.0	0.7	4.5	92.9	1.1	6.2	91.9	0.42	5.6	92.5
II	*EIMi18*	10,446	96.0	2.2	0.2	93.7	2.1	4.5	91.7	0.84	3.2	92.9
	EIMi6	14,555	96.1	1.1	1.5	93.6	2.1	4.7	91.6	0.83	3.4	92.8
	EVM15	10,994	95.8	2.4	0.0	93.5	2.1	4.5	91.5	0.83	3.2	92.7
	SIMf6	14,862	95.4	2.1	0.0	93.4	2.1	4.1	91.5	0.84	2.9	92.6
	V3D15	10,635	96.0	2.5	0.1	93.5	2.3	4.8	91.4	0.87	3.4	92.7
	E3D6	12,589	95.7	2.5	0.0	93.3	2.1	4.5	91.4	0.82	3.3	92.5
	V3D6	13,098	95.9	2.6	0.2	93.2	2.2	4.9	91.2	0.75	3.5	92.5
	EIMi15	12,105	95.4	2.4	0.0	93.1	2.1	4.5	91.1	0.84	3.2	92.3
	EVM6	13,526	95.5	2.7	0.0	92.9	2.1	4.7	91.0	0.82	3.5	92.2
	S3D15	9913	95.8	3.0	0.0	92.9	2.1	5.1	90.9	0.84	3.8	92.1
	S3D18	10,135	96.3	3.6	0.0	92.8	2.2	5.7	90.8	0.85	4.4	92.0
	V3D18	9960	95.9	2.9	0.1	93.0	2.6	5.5	90.6	0.87	3.8	92.2
III	*S3D6*	12,153	95.6	3.4	0.0	92.3	2.1	5.4	90.4	0.82	4.2	91.6
	EVM10_1	11,455	96.4	1.2	3.6	91.8	2.1	6.7	89.9	0.82	5.5	91.1
	VVM15	21,233	96.0	3.5	1.0	91.7	2.3	6.7	89.6	0.97	5.4	90.8
	SIMf18	15,414	96.4	0.9	4.4	91.3	2.3	7.4	89.2	0.89	6.1	90.5
	VIMi18	29,621	95.6	3.6	0.1	92.1	3.5	7.0	88.9	1.17	4.8	91.0
	VVM6	21,926	96.0	4.1	1.9	90.3	2.1	7.9	88.4	0.85	6.7	89.5
	EVM10_2	10,421	96.2	4.7	10.8	81.8	2.1	16.7	80.1	0.81	15.7	81.1

* Plans nomenclature follows the following criteria: first letter for Linac manufacturer, second to third or fourth letters identify technique (see Table 1) and finally the number identifies energy. To discriminate between VMAT plans with single or double arcs, '_1′ or '_2′ was added, respectively. '_fff' identifies the flattening-filter-free mode.

where D_T and d_T are the prescribed dose to the target and the corresponding fraction dose, respectively. See Table 2 for the other parameters.

Then, the LAR for organs in the medium-dose region was calculated following the methodology described in [27] as follows

$$LAR_k^{medium-dose} = \int_{e+L}^{a_{max}} \beta_{EAR-UK,k} \cdot OED_k \cdot exp\left[\gamma_{e,k}(e-30) + \gamma_{a,k} ln\left(\frac{a}{70}\right)\right] \cdot \frac{S(a)}{S(e)} da \quad (6)$$

where k represents the specific organ, γ_e and γ_a are organ-specific parameters depending on the age at exposure e (calculations were carried out for 60 and 80 years) and the attained age a, respectively. a_{max} is the maximum age (100 years), L the latent period for cancer induction and β_{EAR-UK} represents the initial slope of risk transferred to a Western from the risks to the Japanese population. $S(a)/S(e)$ is the probability of surviving to age a conditional on survival to age e. The quantities $S(a)$ were obtained from Anderson and DeTurk [28]. See Table 2 for the other parameters.

For organs total or partially located outside the 5% isodose (the low-dose region), where the dosimetric accuracy of TPS decreases [29], the total equivalent dose was computed using two analytical models for evaluation of the photon [30] and neutron [31] peripheral dose (H_T^γ and H_T^n, respectively). Note that the contribution of neutrons to the dose to organs in the volume close to the field edge (i.e., approximately 2 cm crust around it) is not considered in the calculation of $LAR_k^{medium-dose}$ as is negligible compared to photons.

In the low dose region (< 4 Gy) a different approach for LAR calculation was followed. There are two reasons. The first one is that, to authors' knowledge, for the other more peripheral organs, there are no organ-specific coefficients to feed the dose–response mechanistic model. Then, atomic bomb survivors data became the only available resource. Although survivors and radiotherapy patients have different exposure conditions, some works showed that in the low dose region, the mechanistic models reproduce the Linear Non-Threshold (LNT) [25,32]. The second reason is the lack of dose-volume histogram information for the organs outside the 5% isodose. Therefore, for the low-dose region. LAR was calculated as

$$LAR_k^{low-dose} = \lambda_k \cdot H_{T,k} = \lambda_k \cdot (H_{T,k}^n + H_{T,k}^\gamma) \quad (7)$$

where λ_k is organ-specific incidence risk coefficients from BEIR report [23], in particular, those for males at an age at exposure of 60 in Table 1D2-1.

H_T^γ was estimated using patient and treatment parameters required

by PERIPHOCAL model [30] such as the number of MU of each plan, dose prescription at the isocenter, location of the isocenter (91 cm from the patient head and at 11.4 cm depth), distance from the 50% to 5% isodoses (2 cm measured on a coronal plane containing the isocenter) and patient height (176 cm). Eq. (8) summarises the model implemented in PERIPHOCAL

$$H_T^{\gamma,low-dose}(L, z, f, \epsilon) = \frac{1}{(X_{org} + L) - X_{org}^{'}} \int_{X_{org}^{'}}^{X_{org}+L} PPD(x^{'}, z, f, \epsilon).\, dx^{'} \tag{8}$$

where L is the length of each particular organ, z is the isocenter depth, f is the equivalent square field size (in cm), and ϵ the treatment efficiency parameter (ratio of the dose prescribed to the isocentre and the MU needed to deliver the prescribed dose, relative to the case of the $10 \times 10\,cm^2$ eight open beams used as the reference). The integration limits are chosen as a function of the position of the organ with respect to the treatment beams (details in [30]), and PDD is the photon peripheral dose to a point calculated calculated as follows

$$PPD(x, z, f, \epsilon) = A + \frac{B}{x^2} \epsilon \left(\frac{f}{10}\right)^2 e^{-(\mu_{air} \cdot r_{air} + \mu_{tissue} \cdot r_{tissue})} \tag{9}$$

With x, the cranio-caudal distance from the isocenter to the calculation point, A and B fitted parameters of the model (A = 0003 mSv/UM and B = 17.612 mSv·cm^2/UM), and r_{air} and r_{tissue} the distances traversed by the beam from the vitual source to the calculation point in air and tissue, respectively and are calculated from a simple geometrical approximation as described in [30]). μ_{air} and μ_{tissue} are linear attenuation coefficients for air and soft tissue ($\mu_{air} = 2 \times 10^{-5}\,cm^{-1}$ and $\mu_{tissue} = 2.325\ 10^{-2}\,cm^{-1}$), respectively.

The matlab script for the calculation has been made available as additional material. H_T^n was estimated from the MUs of the plan [31].

4. Results

The minimum dose was usually below 0.5 Sv, except for rectum, bladder and bone marrow, with an average value of 21.7 Sv, 16.3 Sv, and 0.6 Sv, respectively. The total equivalent dose to every peripheral organ for each plan is provided in the supplementary material (Table 1).

Table 3 shows all the biological indexes calculated for all the plans. TCP ranged from 95.4% to 98.0%, the highest values being associated with SBRTs. Average $NTCP_{rectal}$ and $NTCP_{bladder}$ were 1.9% and 1.0%, respectively. $NTCP_{rectal}$ varied from 0.3% for a forward-planned IMRT at 6 and 15MV to 4.7% for the two-arcs10MV VMAT. $NTCP_{bladder}$ ranged from 0.0% for several plans to 10.8% for 10MV VMAT (2 arcs).

SPCR, GCP and UCFCP for each plan are reported for two ages at exposure, 60 and 80 years. Unless stated otherwise, values commented in this section are meant only for 60 years. The reader is referred to the discussion section for comments on the impact of the age at exposure value upon SPCR and final plan ranking. The lowest (1.1%) and the highest (3.5%) SPCR corresponded to the SBRTs and one inverse-planned high energy IMRT plan, respectively. The rate of second solid cancer sites near the radiation portals were 0.5% for rectum and colon and 0.4% for the bladder. Fig. 2a displays average SPCR, $NTCP_{rectal}$, and $NTCP_{bladder}$ values for "modern techniques" (i.e., IMRT, and VMAT), 3DCRT and SBRT split into high and low energy. In Fig. 2b, SPCR by solid cancer site and leukaemia on all the same groups is shown (values provided in the supplementary material (Table II)).

Plans in Table 3 are ranked according to their UCFCP values. The leading plan was 10MV SBRT, which exhibited an extra 15.2% in the probability of uncomplicated cure over the worst ranked plan (10MV VMAT with two arcs). With the aim of posteriorly extract the main features of the best and worst ranked plans, three equally-sized groups were created (I, II, III). General characteristics of each of the three groups were described in terms of the biological indexes (TCP, NTCP, SPCR, GCP) and the therapeutic ratio (i.e., TCP/GCP) (Fig. 3a–c). Additionally, the percentage of plans inside each group with high energy (i.e., ≥10 MV) and those designed with a modern technique were identified inside each group (Fig. 3d).

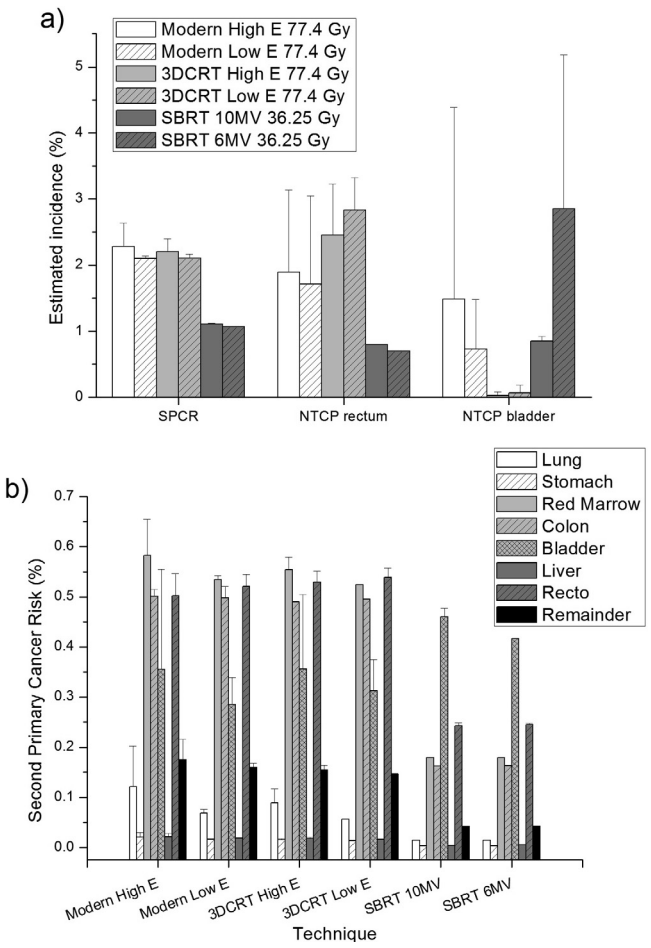

Fig. 2. Average value of SPCR and NTCP as well as SPCR for cancer sites are depicted in a) and b), respectively. SPCR values are for age at exposure = 60y. Error bars display SD.

5. Discussion

A single pelvic CT set (with contours) was selected as a way to focus the analysis on the ranking of a broad range of photon techniques which are currently available to treat PoCa. We did not aim to find the optimal technique for photon RT in PoCa. But instead, to illustrate the relevance of incorporating SCP in the selection of the best plan for the selected anatomy, provided the hypothetical situation in which all the 36 plans were available. A discussion on the values obtained for the different biological indexes compared to clinically or epidemiological data will help to put in context the goodness of the calculations performed.

5.1. TCP and NTCP

It has to be noted that our TCP values were higher than the usually reported proportion of patients who are biochemical or clinical failure free after conventional or altered fractionated RT. This might be related to the fact that our local control rates were calculated on the GVT for which the prescription requirements ensured their coverage to at least 77.4 Gy (indeed, slightly higher prescription dose than in [6]). This choice was driven by the fact that no information on the gradient of clonogenic cell density across the tumour is available and possibly, by

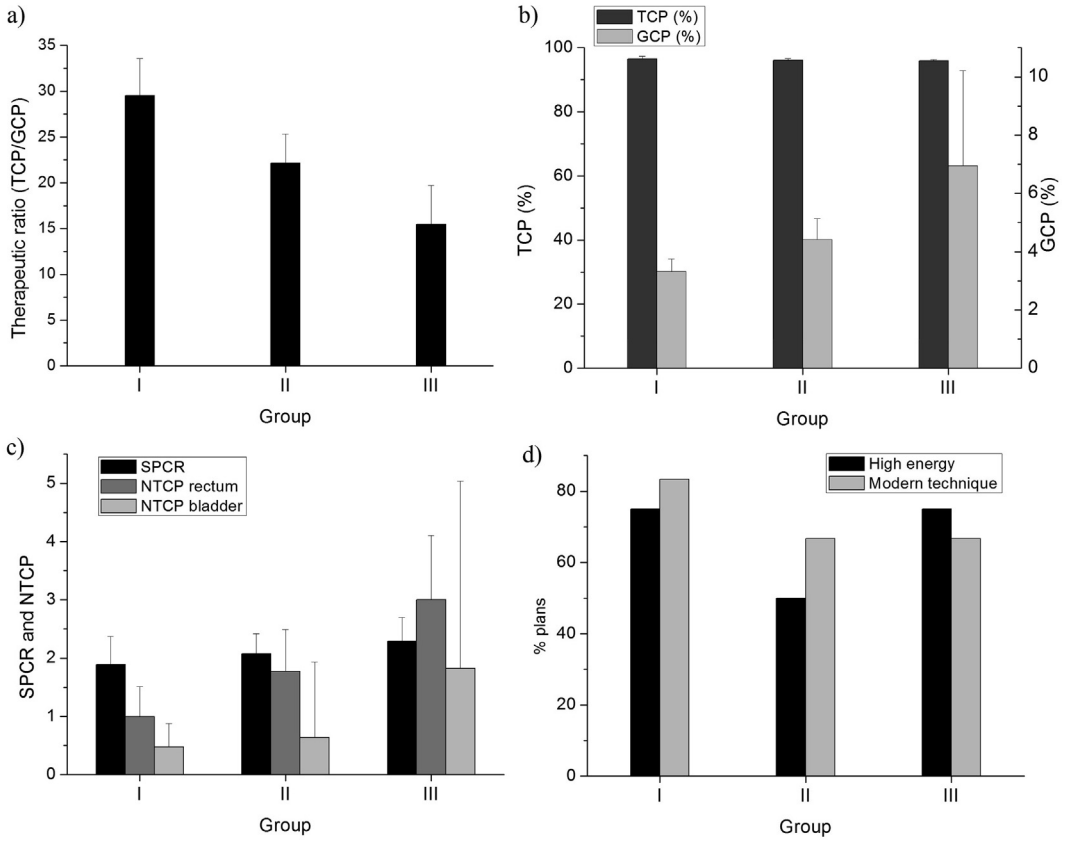

Fig. 3. From a) to c): average values of biological indexes (error bars display SD) of the three groups. In d) distribution of plans according to energy and technique. GCP and SPCR values are for age at exposure = 60y.

assuming that no tumour cells are present outside the GTV, that underestimation of the total number of tumour cells produces the obtained high TCP values. [6]. Another source of uncertainty comes from the values of the biological parameters of the model. A broad range of α/β values for prostate has been reported [33] (from 0.6 Gy to > 10 Gy). However, the assessment of the whole set of radiobiological parameters had not been the primary goal of those clinical studies and, at best, α is reported. Thus, a crude estimation of σ_α and ρ_c is additionally required. Even more, the α values published together with the $\alpha/\beta < 3$ are very small ($\approx 0{,}05\ \mathrm{Gy}^{-1}$) which would imply the use of an extremely low number for the clonogenic cell density in order to reproduce realistic clinical dose–response curves. Our final choice for the value of the parameters represented a wise compromise between a relatively low α/β, plausible values for the other parameters and the generation of sensible tumour control response rates.

Nonetheless, as TCP values for all plans were substantially the same (consistent with the fulfilment of the dose prescription requirements), plan ranking for this patient has not been affected nor our conclusions on the relevance of SCP in plan ranking.

As expected, rectum sparing was better with intensity-modulated techniques than with 3DCRT plans (average $NTCP_{rectal}$ of 2.6% vs 1.7%). However, the opposite was observed for the bladder (1.3% vs 0.1%). The latter result lies in the fact that the parameter n for the bladder is almost zero, indicating that the maximum dose to that organ is critical in determining toxicity. Effectively, the bladder DVH for the EVM10_2 plan, with the highest probability of GU toxicity (10.8%), is below some others, with 0% of estimated toxicity, except by a small volume irradiated above 62 Gy (insert in Fig. 1c). VSB6 also showed a high $NTCP_{bladder}$ (4.5%) as a consequence of the LQ-corrected hot spot (> 78 Gy), which according to [22] is critical for G1 bladder toxicity. Therefore, even the better tailoring of the PTV as with intensity-modulated techniques could let it slip a small hot spot able to raise $NTCP_{bladder}$. Consequently, the range of hot spots traduces in a high standard deviation for $NTCP_{bladder}$ numbers. And yet, all plans met the recommended urinary bladder dose constraints by QUANTEC [16].

5.2. SPCR

Despite databases heterogeneity, the PROBATE groups [2] and Brenneŕs [34] reports agree on an increased risk of solid SPCR following radiation for PoCa (1 in 70 and 1 in 290 for patients followed up for more than ten years for (2) and [34], respectively). Berrington et al. [14] carried out a risk assessment of solid second cancer among PoCa patients finding an approximate total incidence rate of 9% (from which only 8% would be related to radiotherapy [35]). By applying the same 8% to the cumulative incidence of all second primary cancers to Hegemanńs cohort (a population-based study on the Munich cancer registry) [36], SPCR due to RT of 1,3% and 2% after 10 and 20 years, respectively was obtained.

Our numbers show discrete differences in SPCR among plans. Total SPCR ranged from 1.1% to 3.5% with an average of approximately 2%, which decreases to 0,8% for age at exposure = 80y (consistent with the decrease in sensitivity for older patients). For 77.4 Gy techniques, absolute differences in SPCR were smaller. SBRT plans showed at least a twofold decrease (average of 1.1%) (Fig. 2a). The predicted radiation-induced cancer risk benefit from SBRT techniques has been discussed in previous studies [12,37,38].

Our calculations showed that the most frequent second cancers were any form of leukemia, rectal (in the medium-dose region), colon (close to the border of the field) and bladder (lying across the medium- to low-dose region) cancers, in that order (see Fig. 2b) in agreement with [39]. Risks in the medium-dose region, estimated using the mechanistic model by Schneider, represented 40% of all SPCR (in agreement with the spatial distribution described in [40]). A discrepancy was observed

between our calculation and previous findings on $SPCR_{rectal}$ for which no significant increase compared to the healthy population was reported [2,14,34,36,41]. Additionally, Murray et al. [12] predicted 0.6% average $SPCR_{rectal}$ for 6MV VMAT and IMRT (based on the competition model) for the complete rectal DVH (i.e., their study considers SPCRs in in-field tissues). This figure agrees with our estimation (for age at exposure = 60 y and age at exposure = 80 y as in [12]) of 0.5% in the out-of-field region for the 77.4 Gy 6MV IMRT/VMAT plans. When Excess Absolute Risk (EAR) (per 10,000 persons/year) of second malignancies in the in-field rectum (i.e., the whole DVH is considered) was calculated for the techniques and energies analyzed in [12], our values resulted larger (3.7 vs. 2.4, 3.7 vs 2.6 and 3.8 vs. 2.7 for 6MV-VMAT, 6MV-IMRT and 10MV-3DCRT, respectively), most probably reflecting differences in patienťs anatomies. As seen in Fig. 2b, the largest SPCR was associated with any form of leukaemia, an average of 0.5% in agreement with previous population-based studies [42,43]. Nonetheless, others have not found a significant increase in leukaemia rates [34,41].

The small differences found in second solid cancers between high and low energy plans endorse previous results as being similar overall [14]. In our study, and for the case of high energy plans, this was due to the lesser MU (Table 3) required for the higher energy plans (in average, 12,345 vs 15091) which more than offsets the extra neutron dose. Even more, despite concerns on neutron doses, high energy intensity-modulated plans did not appear to increase in excess the average SPCR (2.3% and 2.1% for high and low energies intensity-modulated 77.4 Gy plans, respectively). This difference is almost no existent among 3DCRTs.

We believe that the perception of higher SCPR associated to intensity modulated techniques when delivered using high energy photon beams has less to do with facts but with the lack of analytical models to estimate peripheral dose to organs due to photons and neutrons. That is, the uncertainty might tend to increase the perception of risk. As an example, it was enough to carry out the present exercise to see that wise exploitation of planning capabilities can outweigh the problem of neutron production. Specifically, the same level of SCPR was calculated for IMRT plans with 6 MV (VIMi6) and 15 MV (SIMf15). Moreover, probably a 15MV 3D CFRT would not be questioned as a clinically feasible plan, and yet it can be associated with a high number of MU if, for example, wedges are used. Finally, for “big” patients high energies are probably a better choice which should be considered.

5.3. UCFCP

Plans were ranked according to UCFCP, but if UCP would have been used instead (i.e., ignoring SPCR), no much difference would have been found. Particularly, one-third of the plans would have kept the position (including the best and worst ranked), and another third would have changed one place. That is, provided that adverse effects were considered equally undesirable, this exercise showed that the inclusion of SPCR seemed not to affect the ranking critically. However, far from undermining its value, the present exercise gives some light to the other way valid, concerns on the use of intensity-modulated techniques at high energy which have been possibly biasing the treatment choices. When SPCR was calculated for age at exposure = 80y the ranking suffered a minimal impact, with low energy plans giving way generally to high energy plans, though average value decreased from 2.1% to 0.8%.

The equally-sized groups (Table 3 and Fig. 3) helped to characterise the best/worst plans. As dispersion within TCP values was small (SD = 0.7%), groups differed on the therapeutic ratio (Fig. 3a) due to different GCP (Fig. 3b). Moreover, GCP was mainly controlled by NTCP as distribution of SPCR values was even more uniform (SD = 0.4%) than TCP (Fig. 3c). The proportion of intensity-modulated plans decreased from the group I to III, whereas energies appeared randomly distributed among them (Fig. 3d). This meant that the better sparing of intensity-modulated techniques (decreasing $NTCP_{rectum}$ and SPCR in the medium-dose region) compensated both, the sometimes larger $NTCP_{bladder}$ and the usual larger number of MU (which increases peripheral photons and, at high energy, the additional peripheral neutrons). The best ranked were the 36.25 Gy plans (FF and FFF-10MV as well as the FFF-6MV) (Table 3). Interestingly, the second best plans were two IMRT techniques for Varian, one at 15MV (though Varian shows the highest neutron production [44,45]). Those plans were created using forward planning (as with a class solution [46]) which optimised the requirement of MU.

SBRT plans exhibited the lowest SPCR and a below average $NTCP_{rectal}$ which make them attractive techniques. Nonetheless, they probably demand a more intensive image treatment guidance than, for example, 3DCRT. In the case of ionizing radiation based images for treatment guidance, the additional dose to peripheral organs could dissipate the initially advantageous SPCR gap.

It is also worth stressing that the ranking was performed using a function which equally weighted tumour and dose–response of healthy peripheral organs (though, for example, the severity of G1 bladder and G2 rectal damages are, by definition, different). Nonetheless, the life expectancy of the patient is implicitly considered by the SCPR model used as LAR includes the probability of surviving until attained age considered conditional on survival to the age at exposure. Any other particular scenario regarding clinical judgement (e.g., particular short life expectancy due to a pre-existing disease) could make NTCP more relevant than SPCR, which could be assigned a smaller impact on the global function.

The average values presented here implicitly considered that in our theoretical PoCa population, the 36 possible external beam radiation treatments were used in an equal proportion which has to be born in mind when comparing our average biological indexes with results from epidemiological or theoretical studies. Even more, our study lacks from the large dose prescription ranges seen in a real population and therefore, the impact of dosimetrical variability cannot be addressed. Nevertheless, relative comparisons among techniques can still raise valid conclusions, and absolute estimations should be compatible within reported ranges.

6. Conclusions

We have shown a procedure to estimate the clinical outcome comprehensively, considering altogether tumour control as well as stochastic and determinist radiation side effects. This methodology might aid the choice of the best plan among the options available without the bias induced by preconceived tendencies.

In the case studied, the best plans were the SBRTs which avoided hot spots (> 78 Gy LQ-equivalent) to the bladder. It was also found that SPCR rates were low and very similar across plans (all but two had SPCR between 1.1% and 2.5%), even considering both dose prescription groups. Thus, SPCR did not show a strong impact on plan ranking. High energy intensity-modulated plans did not appear to increase in excess the average SPCR. Even more, the latter ranked among the best provided that the MUs were efficiently managed. From the minimisation of SPCR point of view, all SBRT plans stood out as the most attractive techniques.

Our exercise illustrated that preconceived ideas about the appropriateness of a particular technique might lead to miss perfectly competent plans which a priori were banned by trends possibly nourished by distrust on the unknown.

Declaration of Competing Interest

The authors declare that they have no known competing financial interests or personal relationships that could have appeared to influence the work reported in this paper.

Acknowledgements

Authors want to thank E. Cagni, C. Ghetti, S. Filice and D. Grishchuk for providing some of the plans used for the present study.

Funding

BSN acknowledges the support of Conicyt FONDECYT Regular 2018 (N1181133) and of Pontificia Universidad Católica de Chile [EPB2016, P1702/2017 and "Concurso de Apoyo a Sabáticos Internacionales 2017"]. MRE would like to thank Banco Santander for its support through the grant program "Becas Iberoamérica. Jóvenes Profesores e Investigadores y Alumnos de Doctorado Santander Universidad". These sources of funding allowed academic interchange between Chile and Spain to carry out the collection, data analysis and interpretation as well as for writing the manuscript.

References

[1] Widmark A, Klepp O, Solberg A, Damber J-E, Angelsen A, Fransson P, et al. Endocrine treatment, with or without radiotherapy, in locally advanced prostate cancer (SPCG-7/SFUO-3): an open randomised phase III trial. Lancet (London, England) 2009;373:301–8. https://doi.org/10.1016/S0140-6736(08)61815-2.

[2] Murray L, Henry A, Hoskin P, Siebert F-A, Venselaar J. PROBATE group of GEC ESTRO P group of the G. Second primary cancers after radiation for prostate cancer: a systematic review of the clinical data and impact of treatment technique. Radiother Oncol 2014;110:213–28. https://doi.org/10.1016/j.radonc.2013.12.012.

[3] Dearnaley DP, Khoo VS, Norman AR, Meyer L, Nahum A, Tait D, et al. Comparison of radiation side-effects of conformal and conventional radiotherapy in prostate cancer: a randomised trial. Lancet 1999;353:267–72. https://doi.org/10.1016/S0140-6736(98)05180-0.

[4] Dearnaley DP, Sydes MR, Graham JD, Aird EG, Bottomley D, Cowan RA, et al. Escalated-dose versus standard-dose conformal radiotherapy in prostate cancer: first results from the MRC RT01 randomised controlled trial. Lancet Oncol 2007;8:475–87. https://doi.org/10.1016/S1470-2045(07)70143-2.

[5] S.H. Benedict, K.M. Yenice, D. Followill, J.M. Galvin, W. Hinson, B. Kavanagh, et al. Stereotactic body radiation therapy: The report of AAPM Task Group 101 Fang-Fang Yin, 2010, doi: 10.1118/1.3438081.

[6] Dearnaley D, Syndikus I, Mossop H, Khoo V, Birtle A, Bloomfield D, et al. Conventional versus hypofractionated high-dose intensity-modulated radiotherapy for prostate cancer: 5-year outcomes of the randomised, non-inferiority, phase 3 CHHiP trial. Lancet Oncol 2016;17:1047–60. https://doi.org/10.1016/S1470-2045(16)30102-4.

[7] Allen Li X, Alber Markus, Deasy Joseph O, Jackson Andrew, Ken Jee Kyung-Wook, Marks Lawrence B, Martel Mary K, Mayo Charles, Moiseenko Vitali, Nahum Alan E, Niemierko Andrzej, Semenenko Vladimir A, Yorke Ellen D. The use and QA of biologically related models for treatment planning: short report of the TG-166 of the therapy physics committee of the AAPM: TG-166 report. Med. Phys. 2012;39(3):1386–409. https://doi.org/10.1118/1.3685447.

[8] Chibani O, Ma C-MC. Photonuclear dose calculations for high-energy photon beams from Siemens and Varian linacs. Med Phys 2003;30:1990–2000. https://doi.org/10.1118/1.1590436.

[9] Hall EJ, Wuu CS. Radiation-induced second cancers: the impact of 3D-CRT and IMRT. Int J Radiat Oncol Biol Phys 2003;56:83–8. https://doi.org/10.1016/S0360-3016(03)00073-7.

[10] Kry SF, Salehpour M, Followill DS, Stovall M, Kuban DA, White RA, et al. The calculated risk of fatal secondary malignancies from intensity-modulated radiation therapy. Int J Radiat Oncol Biol Phys 2005;62:1195–203. https://doi.org/10.1016/j.ijrobp.2005.03.053.

[11] Sánchez-Doblado F, Domingo C, Gómez F, Sánchez-Nieto B, Muñiz JL, García-Fusté MJ, et al. Estimation of neutron-equivalent dose in organs of patients undergoing radiotherapy by the use of a novel online digital detector. Phys Med Biol 2012;57. https://doi.org/10.1088/0031-9155/57/19/6167.

[12] Murray LJ, Thompson CM, Lilley J, Cosgrove V, Franks K, Sebag-Montefiore D, et al. Radiation-induced second primary cancer risks from modern external beam radiotherapy for early prostate cancer: impact of stereotactic ablative radiotherapy (SABR), volumetric modulated arc therapy (VMAT) and flattening filter free (FFF) radiotherapy. Phys Med Biol 2015;60:1237–57. https://doi.org/10.1088/0031-9155/60/3/1237.

[13] Sánchez-Nieto B, Romero-Expósito M, Terrón JA, Sánchez-Doblado F, Brenner DJ, Newhauser WD. Uncomplicated and Cancer-Free Control Probability (UCFCP): a new integral approach to treatment plan optimization in photon radiation therapy. Phys Medica 2017;47:35–41. https://doi.org/10.1016/j.ejmp.2017.03.025.

[14] Berrington De Gonzalez A, Wong J, Kleinerman R, Kim C, Morton L, Bekelman JE. Risk of second cancers according to radiation therapy technique and modality in prostate cancer survivors. Int J Radiat Oncol Biol Phys 2015;91:295–302. https://doi.org/10.1016/j.ijrobp.2014.10.040.

[15] Gulliford SL, Foo K, Morgan RC, Aird EG, Bidmead AM, Critchley H, et al. Dose-volume constraints to reduce rectal side effects from prostate radiotherapy: evidence from MRC RT01 trial ISRCTN 47772397. Int J Radiat Oncol Biol Phys 2010;76. https://doi.org/10.1016/j.ijrobp.2009.02.025.

[16] Viswanathan AN, Yorke ED, Marks LB, Eifel PJ, Shipley WU. Radiation dose-volume effects of the urinary bladder. Int J Radiat Oncol Biol Phys 2010;76:116–22. https://doi.org/10.1016/j.ijrobp.2009.02.090.

[17] Sanchez-Nieto B, Nahum AE. Bioplan: software for the biological evaluation of radiotherapy treatment plans. Med Dosim 2000;25. https://doi.org/10.1016/S0958-3947(00)00031-5.

[18] Sanchez-Nieto B, Nahum AE. The delta-TCP concept: a clinically useful measure of tumor control probability. Int J Radiat Oncol Biol Phys 1999;44. https://doi.org/10.1016/S0360-3016(99)00029-2.

[19] Lyman JT. Complication probability as assessed from dose-volume histograms. Radiat Res Suppl 1985;8:S13–9.

[20] Kutcher GJ, Burman C. Calculation of complication probability factors for non-uniform normal tissue irradiation: the effective volume method. Int J Radiat Oncol Biol Phys 1989;16:1623–30. https://doi.org/10.1016/0360-3016(89)90972-3.

[21] Michalski JM, Gay H, Jackson A, Tucker SL, Deasy JO. Radiation dose-volume effects in radiation-induced rectal injury. Int J Radiat Oncol Biol Phys 2010;76:123–9. https://doi.org/10.1016/j.ijrobp.2009.03.078.

[22] Cheung MR, Tucker SL, Dong L, de Crevoisier R, Lee AK, Frank S, et al. Investigation of bladder dose and volume factors influencing late urinary toxicity after external beam radiotherapy for prostate cancer. Int J Radiat Oncol Biol Phys 2007;67:1059–65. https://doi.org/10.1016/j.ijrobp.2006.10.042.

[23] National Research Council (U.S.). Committee to Assess Health Risks from Exposure to Low Level of Ionizing Radiation. Health risks from exposure to low levels of ionizing radiation : BEIR VII, Phase 2. National Academies Press; 2006.

[24] Schneider U, Zwahlen D, Ross D, Kaser-Hotz B. Estimation of radiation-induced cancer from three-dimensional dose distributions: Concept of organ equivalent dose. Int J Radiat Oncol 2005;61:1510–5. https://doi.org/10.1016/j.ijrobp.2004.12.040.

[25] Schneider U. Mechanistic model of radiation-induced cancer after fractionated radiotherapy using the linear-quadratic formula. Med Phys 2009;36:1138–43. https://doi.org/10.1118/1.3089792.

[26] Schneider U, Sumila M, Robotka J. Site-specific dose-response relationships for cancer induction from the combined Japanese A-bomb and Hodgkin cohorts for doses relevant to radiotherapy. Theor Biol Med Model 2011;8:27. https://doi.org/10.1186/1742-4682-8-27.

[27] Fuji H, Schneider U, Ishida Y, Konno M, Yamashita H, Kase Y, et al. Assessment of organ dose reduction and secondary cancer risk associated with the use of proton beam therapy and intensity modulated radiation therapy in treatment of neuroblastomas. Radiat Oncol 2013;8:255. https://doi.org/10.1186/1748-717X-8-255.

[28] Anderson RN, DeTurk PB. United States life tables, 1999. Natl Vital Stat Rep 2002;50:1–39.

[29] Bezak E, Takam R, Yeoh E, Marcu LG. The risk of second primary cancers due to peripheral photon and neutron doses received during prostate cancer external beam radiation therapy. Phys Medica 2017;42:253–8. https://doi.org/10.1016/j.ejmp.2017.02.018.

[30] Sánchez-Nieto B, Elfar R, Irazola L, Romero-Expósito M, Lagares JI, Mateo JC, et al. Analytical model for photon peripheral dose estimation in radiotherapy treatments. Biomed Phys Eng Express 2015;1. https://doi.org/10.1088/2057-1976/1/4/045205.

[31] Irazola L, Terrón JA, Sánchez-Nieto B, Roberto B. Sánchez-Doblado F. Peripheral equivalent neutron dose model implementation for radiotherapy patients. Phys Medica 2017;42. https://doi.org/10.1016/j.ejmp.2017.03.018.

[32] Shuryak I, Hahnfeldt P, Hlatky L, Sachs RK, Brenner DJ. A new view of radiation-induced cancer: integrating short- and long-term processes. Part II: second cancer risk estimation. Radiat Environ Biophys 2009;48:275–86. https://doi.org/10.1007/s00411-009-0231-2.

[33] van Leeuwen CM, Oei AL, Crezee J, Bel A, Franken NAP, Stalpers LJA, et al. The alfa and beta of tumours: a review of parameters of the linear-quadratic model, derived from clinical radiotherapy studies. Radiat Oncol 2018;13:96. https://doi.org/10.1186/s13014-018-1040-z.

[34] Brenner DJ, Curtis RE, Hall EJ, Ron E. Second malignancies in prostate carcinoma patients after radiotherapy compared with surgery. Cancer 2000;88:398–406. https://doi.org/10.1002/(SICI)1097-0142(20000115)88:2<398::AID-CNCR22>3.0.CO;2-V.

[35] De Gonzalez AB, Curtis RE, Kry SF, Gilbert E, Lamart S, Berg CD, et al. Proportion of second cancers attributable to radiotherapy treatment in adults: a cohort study in the US SEER cancer registries. Lancet Oncol 2011;12:353–60. https://doi.org/10.1016/S1470-2045(11)70061-4.

[36] Hegemann N-S, Schlesinger-Raab A, Ganswindt U, Hörl C, Combs SE, Hölzel D, et al. Risk of second cancer following radiotherapy for prostate cancer: a population-based analysis. Radiat Oncol 2017;12:2. https://doi.org/10.1186/s13014-016-0738-z.

[37] Schneider U, Besserer J, Mack A. Hypofractionated radiotherapy has the potential for second cancer reduction. Theor Biol Med Model 2010;7:4. https://doi.org/10.1186/1742-4682-7-4.

[38] Irazola L, Sánchez-Nieto B, García-Hernández MT, Terrón JA, Roselló J, Ortiz-Seidel M, et al. 10-MV SBRT FFF irradiation technique is associated to the lowest peripheral dose: the outcome of 142 treatment plans for the 10 most common tumour locations. Radiat Prot Dosimetry 2019. https://doi.org/10.1093/rpd/ncy292.

[39] Wallis CJD, Mahar AL, Choo R, Herschorn S, Kodama RT, Shah PS, et al. Second malignancies after radiotherapy for prostate cancer: systematic review and meta-analysis. BMJ 2016;352:i851. https://doi.org/10.1136/bmj.i851.

[40] Diallo I, Haddy N, Adjadj E, Samand A, Quiniou E, Chavaudra J, et al. Frequency distribution of second solid cancer locations in relation to the irradiated volume among 115 patients treated for childhood cancer. Int J Radiat Oncol Biol Phys

2009;74:876–83. https://doi.org/10.1016/j.ijrobp.2009.01.040.
[41] Neugut Alfred I. Bladder carcinoma and other second malignancies after radiotherapy for prostate carcinoma. Cancer 1997;79:1600–5.
[42] Wang R, Zeidan AM, Yu JB, Soulos PR, Davidoff AJ, Gore SD, et al. Myelodysplastic syndromes and acute myeloid leukemia after radiotherapy for prostate cancer: a population-based study. Prostate 2017;77:437–45. https://doi.org/10.1002/pros.23281.
[43] Reddy CA, Ciezki JP, Tiu RV, Advani AS, Saunthararajah Y, Maciejewski JP, et al. Risk Of Acute and Chronic Leukemias Following Radiation Treatment For Locoregional Prostate Cancer In The United States Over 35-Years. Blood 2013;122.
[44] Expósito MR, Sánchez-Nieto B, Terrón JA, Domingo C, Gómez F, Sánchez-Doblado F. Neutron contamination in radiotherapy: estimation of second cancers based on measurements in 1377 patients. Radiother Oncol 2013;107. https://doi.org/10.1016/j.radonc.2013.03.011.
[45] Romero-Expósito M, Sánchez-Nieto B, Terrón JA, Lopes MC, Ferreira BC, Grishchuk D, et al. Commissioning the neutron production of a Linac: development of a simple tool for second cancer risk estimation. Med Phys 2015;42. https://doi.org/10.1118/1.4903525.
[46] Peulen H, Hanbeukers B, Boersma L, van Baardwijk A, van den Ende P, Houben R, et al. Forward intensity-modulated radiotherapy planning in breast cancer to improve dose homogeneity: feasibility of class solutions. Int J Radiat Oncol 2012;82:394–400. https://doi.org/10.1016/j.ijrobp.2010.09.005.